COMPARISON OF BEAM TRANSPORT SIMULATIONS TO MEASUREMENTS AT THE LOS ALAMOS PROTON STORAGE RING

C. Wilkinson, F. Neri, D. H. Fitzgerald, B. Blind, R. Macek, M. Plum, O. Sander, H.A. Thiessen,
Los Alamos National Laboratory, Los Alamos, NM 87544

Abstract

The ability to model and simulate beam behavior in the Proton Storage Ring (PSR) of the Los Alamos Neutron Science Center (LANSCE) is an important diagnostic and predictive tool. This paper gives the results of an effort to model the ring apertures and lattice and use beam simulation programs to track the beam. The results are then compared to measured activation levels from beam loss in the ring. The success of the method determines its usefulness in evaluating the effects of planned upgrades to the Proton Storage Ring.

1 SIMULATION

For the model, the dimensions and positions of the PSR beam line elements were obtained from drawings and documentation and were verified by measurements wherever possible. Aperture dimensions included as-built variations, if known. The resulting DIMAD lattice geometry was checked against a 2-d computer layout of the ring. One unverified point remained after this effort: a limiting aperture in the vacuum pipe of the insertion magnet and ring bender, SRBM01. Loss patterns do not indicate that such a restriction exists.

The PSR clear apertures on either side of the beam pipe center are plotted in Figure 1 and the minimum of the apertures on either side is plotted in Figure 2. The smallest apertures in the horizontal direction are found in the extraction kickers (2.58 and 2.90 cm), the extraction septum magnet (4.52 cm), and the unverified vacuum chamber aperture in bender SRBM01 (2.52 cm). For the rest of the ring, the minimum horizontal apertures (4.78 cm) are in the Beam Position Monitors (BPM's) in the quadrupoles and are close to the value for the ring dipole magnets. The horizontal apertures are widest in the beam elements that must handle both circulating and incoming or exiting beams. In the vertical direction, the smallest apertures are in the special vacuum chambers in the ring dipole magnets which must also accommodate the injected (SRBM01, 4.63 cm), unstripped (SRBM11, 4.26 cm), and extraction beams (kickers, 4.34 cm). The remaining ring dipoles and the QU BPM's have the next smallest apertures (4.73 cm).

The beam envelopes were generated by tracking particles in ACCSIM and then using the emittances containing a chosen beam fraction in a DIMAD simulation. The ACCSIM simulation included injection halo, wide-angle Coulomb scattering, momentum spread, and apertures. Beam parameters and characteristics are included in Table 1. For the present PSR, emittances containing 99.95% of the beam tracked by ACCSIM were used in the DIMAD simulation. The momentum spread, $\Delta p/p$, was found to be 0.32%. This includes RF effects of the buncher and is consistent with what is actually seen in operation.

The simulated PSR beam envelopes are plotted inside the clear apertures in Figure 1. The ratio of the minimum clear aperture to beam size is plotted in Figure 2. With the

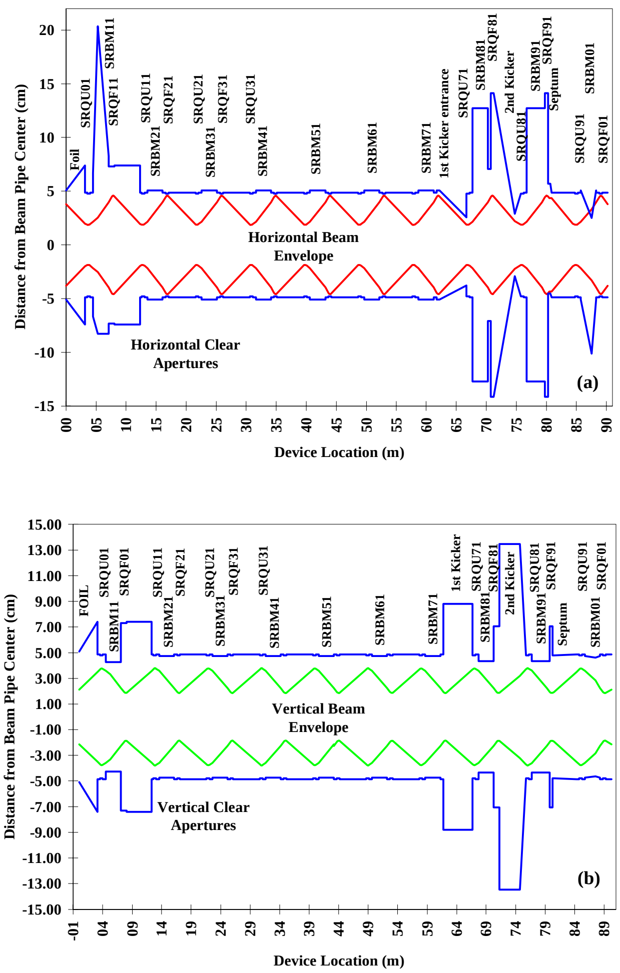

Figure 1(a) and (b). The horizontal and vertical beam envelopes plotted inside the physical clear aperture for the present Proton Storage Ring.

0-7803-4376-X/98/$10.00 © 1998 IEEE

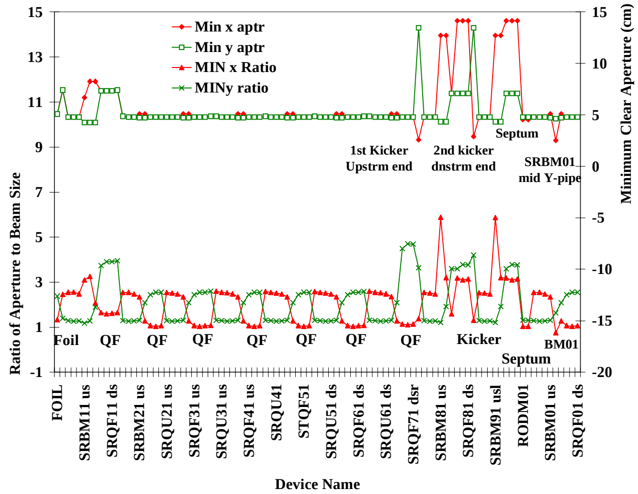

Figure 2. Minimum physical clear apertures and minimum aperture to beam ratios for the present Proton Storage Ring.

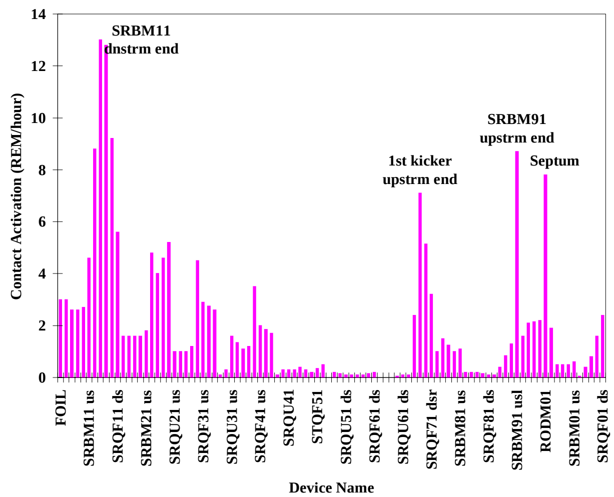

Figure 3. Average measured activation on contact for the present PSR.

exception of the questionable aperture in SRBM01, the limiting aperture for the PSR is in the extraction septum magnet, as given by the aperture ratio of 1.039 in the horizontal direction. The focusing quadrupoles horizontal aperture ratios are only slightly larger, at 1.043, followed by the extraction kickers, at 1.11 and 1.31 respectively. The limiting apertures are distributed around the ring, with no aperture significantly more limiting than any other. Particles reaching a large radius will be lost at the first limiting aperture they encounter and are therefore likely to be lost close to their point of generation.

2 COMPARISON TO MEASUREMENT

A comparison of loss patterns in the PSR corroborates the model of distributed limiting apertures. The averages of several contact measurements of component activation taken over the last five years are plotted in Figure 3. The losses in the injection region are known to come from nuclear scattering, wide-angle coulomb scattering, injection beam halo, and excited H^o states that strip in the first bender field. Particles from these effects are generated at or near the stripper foil. The activation pattern shows that the major injection losses occur in the first four sections of the ring, with peaks at the limiting aperture quadrupole magnets. The large peak in the first bender, SRBM11, is caused primarily by excited H^o's that strip in SRBM11. The upstream apertures shadow the later limiting apertures, so fewer losses are seen in sections five and six.

Activation in the extraction region follows a similar pattern. Although some of the losses are not completely understood, the majority come from beam halo, extracted beam tails, beam in the gap, and unextracted beam. The activation peaks occur at the limiting apertures: the front end of the first kicker, the exit of the second kicker and the entrance of the following ring bender, and the septum magnet. Activation after the unverified constriction in the

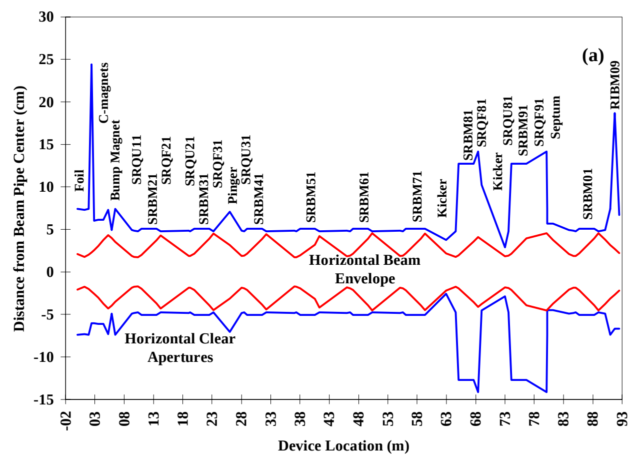

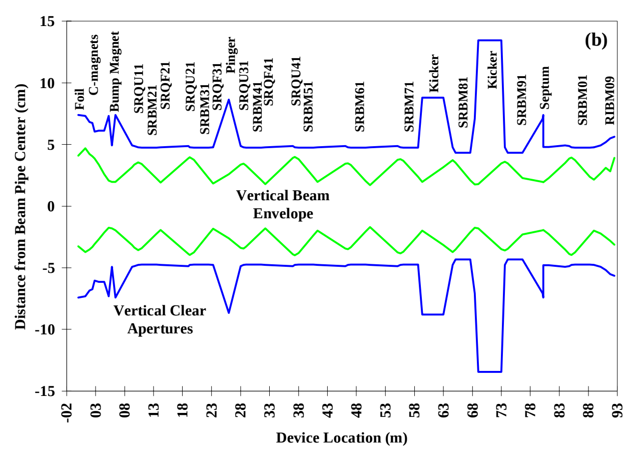

Figure 4 (a) and (b). The horizontal and vertical beam envelopes plotted inside the physical clear aperture for the planned LRIP improvements.

bender, SRBM01, is not consistent with the assumed narrowness of the beam pipe, which in any case will be changed for the LRIP improvement.

3 APPLICATION TO IMPROVEMENTS

The same type of modeling and analysis was applied to the planned upgrade of the ring injection, which is part of the LANSCE Reliability Upgrade Improvement Project (LRIP) scheduled for installation in late 1997. The improvements include direct H^- injection, better matching of the injected beam to the ring acceptance, fewer foil traversals achieved by vertical bumping of the circulating beam and increased vertical beam size, thicker foil, and a change to C-magnets just downstream of the foil. The majority of these changes are intended to reduce ring losses by reducing the number of foil traversals per proton. The present and post-LRIP beam parameters are listed in Table 1. The emittance used for the post-LRIP beam included a slightly larger beam fraction, 99.99%, than that used for the present PSR beam. The results of the analysis are plotted in Figures 4 and 5.

The same pattern of distributed limiting apertures is seen for the LRIP analysis as for the present PSR. The septum aperture ratio is the same and the ratios at the limiting focusing quadrupoles are slightly improved to an average of 1.08. A vertical bump magnet in section 1 becomes the first limiting aperture after the stripper foil, but its aperture equals that of the other limiting apertures. Thus, the LRIP improvements do not introduce new limiting apertures or decrease the aperture ratios, even when more beam is included in the LRIP beam envelope than for the PSR.

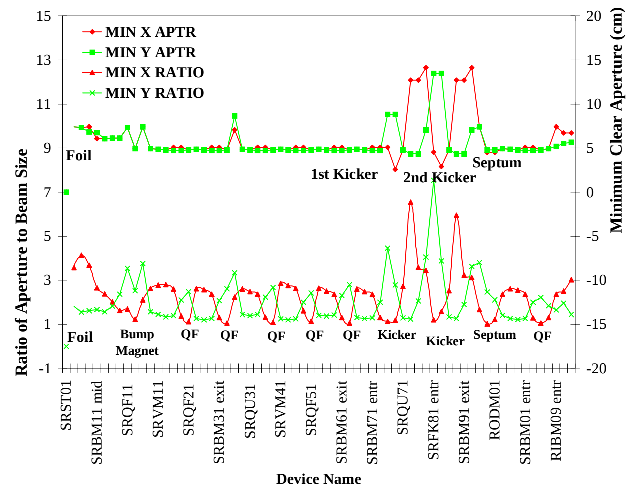

Figure 5. Minimum physical clear apertures and aperture to beam ratios for the LRIP Proton Storage Ring.

4 SUMMARY

The modeling of the present Los Alamos Proton Storage Ring gives aperture to beam size ratios that are consistent with the losses as indicated by contact activation measurements. The success in matching present limiting apertures to losses implies that the method is useful in analyzing planned improvements to the PSR. An analysis of the LANSCE Reliability Improvement Project predicts that there are no major changes in the distribution and size of the limiting apertures, indicating that the improvements have not made the loss situation worse due to the introduction of new limiting apertures.

Table 1. Parameters for the present PSR and the planned LRIP improvements.

	PSR **75 μA @ 20 Hz, 250 ns**	**LRIP** **100 μA @ 20 Hz; 250 ns**
Injection Point Lattice	$\alpha_x = 1.891$, $\beta_x = 9.151$ m $\alpha_y = -0.705$, $\beta_y = 4.560$ m	$\alpha_x = 0.629$, $\beta_x = 2.776$ m $\alpha_y = -1.423$, $\beta_y = 10.931$ m
Injected Beam Emittance	$\varepsilon_x = 7.2$, $\varepsilon_y = 4.20$ (4 σ) mm-mrad	$\varepsilon_x = 3.2$, $\varepsilon_y = 3.2$ (4 σ) mm-mrad
Injected Beam dp/p	36% 0.037 $\Delta p/p$ & 64% 0.063% $\Delta p/p$	36% 0.037 $\Delta p/p$ & 64% 0.063% $\Delta p/p$
Bumping	none	$y^1 = 16.0$ mm, $y^{1\prime} = 2.2$ mrad to 0,0 in 825 μs
Horiz. Accept. Def. Apert.	47.8 mm at Quads; 44.9 mm at sept.	47.8 mm at Quads; 44.9 mm at septum
Vert. Accept. Def. Apert.	47.8 mm at center of Quads	47.8 mm at center of Quads
RF Buncher Voltage	8 kV at 2.8 MHz, ramped from 4 kV	10.5 kV at 2.8 MHz, ramped from 6 kV
Frac. of Beam missing Foil	1.25% plus 7.4% through foil	2.56% plus 0.58% through foil
Tunes	$\nu_x = 3.172$, $\nu_y = 2.142$	$\nu_x = 3.172$, $\nu_y = 2.142$
Max. Tune Depressions	$\Delta\nu_x = -0.158$; $\Delta\nu_y = -0.125$; $2.20\text{x}10^{13}$p	$\Delta\nu_x = -0.071$; $\Delta\nu_y = -0.106$; $3.12\text{x}10^{13}$ p
Stored Beam 95% Emitt.,	$\varepsilon_x = 27.0$, $\varepsilon_y = 39.0$ mm-mrad	$\varepsilon_x = 35.0$, $\varepsilon_y = 49.0$ mm-mrad
Stored Beam 95% $\Delta p/p$	±0.32%	±0.34%
Foil Hits/Proton	307.4 (650 μsec Injection)	35.0 (825 μsec Injection)
Stored beam losses (scatt.)	0.152% multiple; 0.105% nuclear	0.0244 ±0.005% mult.; 0.0217 % nucl.
Excited H^0; Extract. Losses	0.259%; 0.05% respectively	0.048%; 0.0078% respectively